frontiers in Plant Science

ORIGINAL RESEARCH
published: 16 September 2021
doi: 10.3389/fpls.2021.726538

Increased CO_2 Relevant to Future Ocean Acidification Alleviates the Sensitivity of a Red Macroalgae to Solar Ultraviolet Irradiance by Modulating the Synergy Between Photosystems II and I

*Di Zhang[1], Juntian Xu[2], Sven Beer[3], John Beardall[1,4], Cong Zhou[1] and Kunshan Gao[1]**

[1]State Key Laboratory of Marine Environmental Science & College of Ocean and Earth Sciences, Xiamen University, Xiamen, China, [2]Jiangsu Key Laboratory of Marine Bioresources and Environment, Jiangsu Ocean University, Lianyungang, China, [3]Department of Plant Sciences and Food Security, Faculty of Life Sciences, Tel Aviv University, Tel Aviv, Israel, [4]School of Biological Sciences, Monash University, Clayton, VIC, Australia

OPEN ACCESS

Edited by:
Jan de Vries, University of Göttingen, Germany

Reviewed by:
Gregor Christa, University of Wuppertal, Germany
Mattia Pierangelini, University of Liège, Belgium

***Correspondence:**
Kunshan Gao
ksgao@xmu.edu.cn

Specialty section:
This article was submitted to Marine and Freshwater Plants, a section of the journal Frontiers in Plant Science

Received: *17 June 2021*
Accepted: *16 August 2021*
Published: *16 September 2021*

Citation:
Zhang D, Xu J, Beer S, Beardall J, Zhou C and Gao K (2021) Increased CO_2 Relevant to Future Ocean Acidification Alleviates the Sensitivity of a Red Macroalgae to Solar Ultraviolet Irradiance by Modulating the Synergy Between Photosystems II and I. Front. Plant Sci. 12:726538. doi: 10.3389/fpls.2021.726538

While intertidal macroalgae are exposed to drastic changes in solar photosynthetically active radiation (PAR) and ultraviolet radiation (UVR) during a diel cycle, and to ocean acidification (OA) associated with increasing CO_2 levels, little is known about their photosynthetic performance under the combined influences of these drivers. In this work, we examined the photoprotective strategies controlling electron flow through photosystems II (PSII) and photosystem I (PSI) in response to solar radiation with or without UVR and an elevated CO_2 concentration in the intertidal, commercially important, red macroalgae *Pyropia* (previously *Porphyra*) *yezoensis*. By using chlorophyll fluorescence techniques, we found that high levels of PAR alone induced photoinhibition of the inter-photosystem electron transport carriers, as evidenced by the increase of chlorophyll fluorescence in both the J- and I-steps of Kautsky curves. In the presence of UVR, photoinduced inhibition was mainly identified in the O_2-evolving complex (OEC) and PSII, as evidenced by a significant increase in the variable fluorescence at the K-step (F_k) of Kautsky curves relative to the amplitude of F_J–F_o (W_k) and a decrease of the maximum quantum yield of PSII (F_v/F_m). Such inhibition appeared to ameliorate the function of downstream electron acceptors, protecting PSI from over-reduction. In turn, the stable PSI activity increased the efficiency of cyclic electron transport (CET) around PSI, dissipating excess energy and supplying ATP for CO_2 assimilation. When the algal thalli were grown under increased CO_2 and OA conditions, the CET activity became further enhanced, which maintained the OEC stability and thus markedly alleviating the UVR-induced photoinhibition. In conclusion, the well-established coordination between PSII and PSI endows *P. yezoensis* with a highly efficient photochemical performance in response to UVR, especially under the scenario of future increased CO_2 levels and OA.

Keywords: chlorophyll fluorescence, CO_2 enrichment, ocean acidification, photosystems II and I, photoinhibition, *Pyropia yezoensis*, ultraviolet-radiation

INTRODUCTION

Living in the intertidal zone, macroalgae are often exposed to periodic harsh light fluctuations and air exposure associated with changes in tide levels. High levels of solar irradiance can significantly decrease photosynthesis and growth rates in macroalgae (Aline et al., 2006; Martin and Gattuso, 2009; Ji and Gao, 2020), while limited light would entail an insufficient energy supply and thus decrease photosynthesis and growth. Under limited light conditions, longer wavelengths within the range of ultraviolet radiation (UVR, 280–400 nm), generally considered to be detrimental to aquatic ecosystems, can be used as light energy for photosynthesis (Gao et al., 2007). Moderate levels of UVA (315–400 nm) are beneficial for carbon fixation in several macroalgae (Gao and Xu, 2008; Xu and Gao, 2010), and can also act as a signal to stimulate the activity of carbonic anhydrase and nitrate reductase (Viñegla et al., 2006), or prompt morphological development during germination of conchospores (Jiang et al., 2007). Furthermore, the effects of UVR also depend strongly on interactions with other environmental factors. For example, increased ocean temperatures result in stratification and shoaling of the upper mixed layer and thus expose organisms to increased levels of solar photosynthetically active radiation (PAR) and UVR (Häder and Barnes, 2019 and reference therein), and the global warming-induced melting of ice and snow would also aggravate the transmission of UVR and increase UVR exposure in polar regions (Williamson et al., 2019; Neale et al., 2021 and references therein). These interactive effects control the levels of exposure of macroalgae to UVR, and may modulate their photosynthetic performance, production of photoprotective compounds and/or repair mechanisms in response to UVR (see the review by Ji and Gao, 2020 and references therein).

As a consequence of anthropogenic CO_2 emissions, the atmospheric CO_2 concentration has been predicted to increase to above 1,000 μatm by the end of this century (e.g., IPCC, 2014). In addition to possible direct effects of higher aqueous CO_2, this will also result in an increase in proton concentration in the seawater (a drop in pH from 8.1 to 7.8), known as ocean acidification (OA). A number of previous studies have shown that OA hindered calcification processes (Gao et al., 1993; Semesi et al., 2009; Gao and Zheng, 2010; Büdenbender et al., 2011) and thus exposed calcified algae to more UVR exposure. In contrast, the elevated availability of dissolved inorganic carbon (DIC) in seawater has been reported to stimulate both photosynthesis and growth in a number of non-calcified macroalgae such as in *Pyropia* sp. (Gao et al., 1991; Zhang et al., 2020), *Palmaria* sp. (Beer and Koch, 1996), *Gloiopeltis* sp., *Gigartina* sp. (Zou and Gao, 2005), *Gracilaria* sp. (Andría et al., 1999, 2001), *Hypnea* sp. (Suárez-Álvarez et al., 2012), and *Ellisolandia* sp. (Korbee et al., 2014). In addition, the increased DIC would also down-regulate the CO_2-concentrating mechanisms (CCMs), which utilize HCO_3^- to compensate for the limitation of CO_2 in seawater and maintain high intracellular CO_2 levels for photosynthesis and growth of the macroalgae (e.g., a green algae *Ulva prolifera* in Xu and Gao, 2012, and a red algae *Pyropia yezoensis* in Li et al., 2016). Since down-regulation of CCMs is known to save operational energy cost (Raven et al., 2014 and references therein), the energy savings can either stimulate algal growth under low light and increase the risk of photoinhibition under high light (especially with the presence of UVR; see the review by Gao et al., 2019 and references therein).

Pyropia (previously known as *Porphyra*; Rhodophyta), an economically important marine crop worth ~US$1.3 billion per year (Blouin et al., 2011), has been widely cultivated in both China and other Asian countries. Previously, we showed that UVR inhibited both carbon assimilation and growth of *P. yezoensis*, while elevated CO_2 exhibited a positive effect and participated in the alleviation of the UVR-induced inhibition (Zhang et al., 2020). In that work, increases of non-photochemical quenching (NPQ) and UV-absorbing compounds (UVACs) were suggested to dissipate and/or absorb the excess energy originating from UVR, while little attention was paid to the transfer of such absorbed energy. In red algae, phycobilisomes (PBS) form the light-harvesting antennae on the outer surface of thylakoid membranes, in the proximity of photosystem II (PSII), the specific mechanisms for this are unclear but may involve state transitions or mobility of PBS, redistributing the energy between the two photosystems and thus altering photosynthetic electron transport and supply of energy for CO_2 fixation and reduction (Su et al., 2010 and references therein). Moreover, regulation of photosynthetic electron transport, e.g., *via* alternative electron transport chains, including cyclic electron transport (CET) around photosystem I PSI, photorespiration and the water-water cycle along with reactive oxygen species (ROS)-scavenging systems, has also been supposed to protect photosynthetic systems from photoinhibition/photodamage (Eberhard et al., 2008 and references therein, Miyake, 2010). In *P. yezoensis*, CET has been verified to play a vital role in photoprotection when thalli suffered from dehydration (Gao and Wang, 2012), severe salt stress (Lu et al., 2016; Yu et al., 2018), and irradiance stress (Niu et al., 2016). The active CET not only participates in NPQ, but also alleviates the over-reduction of plastoquinone and, thus, balance the redox state of the photosynthetic electron transport chain (Miyake, 2010).

In the present study, effects of OA and UVR on the photosynthetic performance of *P. yezoensis* were investigated by growing these algae under incident solar radiation with or without UVR at ambient and elevated CO_2 concentrations projected for future OA by the end of 2100. While high CO_2 and the concomitant OA may have separate effects on algal physiology in nature (Hurd et al., 2020), technically, it is hard to distinguish the specific effects of pH or CO_2. Moreover, pH and CO_2 covary oppositely even in algal blooms or with progressive OA, thus we did not attempt to disentangle the interactions between these two variables. Our aims are 1) characterized the electron transport flux from PSII to PSIl, 2) examined an alternative electron sink, i.e., CET; and 3) evaluated the coordination between PSII and PSI, under the influences of UVR and OA.

MATERIALS AND METHODS

Experimental Treatments and Measurements of UV Irradiance and pH

Thalli of *P. yezoensis* (Ueda) M.S.Hwang & H.G.Choi were collected from rafts offshore of Gaogong Island (34°43′31′ N, 119°31′57′ E), Lianyungang, Jiangsu Province, China, on December 12, 2017, and transported to the laboratory in a cooled Styrofoam box within 2 h. Following rinsing, thalli of ~0.05 *g* fresh weight were grown outdoors for 9 days in 1 L open-ended quartz tubes filled with natural seawater, which were partly immersed in a flow-through water bath to maintain the seawater temperature at 8 ± 1°C. The seawater in each tube was continuously aerated (300 ml per min) with air containing 400 ± 20 or 1,000 ± 50 μatm CO_2, and was renewed every day. The low-CO_2 air was directly obtained with an air pump while the high-CO_2 level was obtained from a CO_2 enricher (HP 1000 G-D, Ruihua Instruments, Wuhan, China), which controls the CO_2 concentration with less than 5% variation. Different radiation treatments were achieved by covering the quartz tubes with Ultraphan film 395 (UV Opak, Digefra, Munich, Germany), Folex 320 film (Montagefolie, Folex, Dreieich, Germany), or Ultraphan film 295 (Digefra), respectively, so that the thalli were exposed to irradiances above 395 nm (PAR alone), above 320 nm (PA, PAR + UVA) and above 295 nm (PAB, PAR + UV-A + B), respectively. Considering the low density of algal blades in the tubes, the self-shading in our present study can be considered minimal. Measurements of photochemical activities (see below) were carried out around 14:00 on the 10th day of treatments. A total of 18 tubes containing different individual thalli were used for measurements, and three independent thalli were used as replicates for each parameter. According to published papers (Mercado et al., 1999; Zou, 2005; Chen et al., 2016, 2017), and also based on our previous experience (Zou et al., 2003; Xu and Gao, 2008, 2010), 10 days culture is enough for full acclimation of the photosynthetic and other biochemical traits in *Pyropia* spp. and other tested marine macroalgae.

The pH_{NBS} was measured at the end of each day by a pH meter (pH 700, Eutech Instruments, Singapore) equipped with an Orion® 8102BN Ross combination electrode (Thermo Electron Co., United States), which was calibrated with NBS standard buffers every day during the experiment (Thermo Fisher Scientific Inc., United States). Total alkalinity (TA) was measured with a TA analyzer (AS-ALK1, Apollo SciTech, United States) by Gran acidimetric titrations. The values of other carbonate chemistry parameters (total inorganic carbon concentration, TIC, bicarbonate and carbonate ions) were calculated by the Excel program CO2SYS (Pierrot et al., 2006) according to the measured values of TA and pH_{NBS}.

The incident solar irradiances were continuously monitored and recorded every minute by a broadband solar radiometer (EKO Instruments Co., LTD, Japan), which has three separate channels, for (PAR, 400–700 nm), UVA (315–400 nm), and UVB (280–315 nm), respectively.

Before the final measurements, the *in situ* diurnal variations (daytime) of pH and CO_2 were measured. These results showed that the total alkalinity (TA) was around ~2,400 μm throughout the day, pH ranged from ~8.2 to 8.4 and the dissolved CO_2 ranged from about 10 to 13 μm. The maximal and daily average PAR values during the experimental period were 812.6 ± 57.4 and 186.1 ± 35.1 μmol photons m^{-2} s^{-1}, respectively, while the corresponding values for UVA were 8.1 ± 0.7 and 1.9 ± 0.3 W m^{-2}, and that for UVB 0.3 ± 0.03 and 0.1 ± 0.01 W m^{-2}. PAR, UVA and UVB levels were 635 μmol photons m^{-2} s^{-1} and 6.5 and 0.2 W m^{-2}, respectively, when the following parameters were measured at 14:00 on the 10th day. During the experiment, the enhanced CO_2 level (from 400 to 1000 μatm in the air phase) resulted a pH drop from 8.24 ± 0.03 to 7.92 ± 0.03 ($n = 27$). While TA remained unaltered, the TIC increased from 2,131 ± 20 to 2,310 ± 20 μm and that of CO_2 from 12 ± 1 to 28 ± 3 μm ($n = 27$) under the high-CO_2 treatment.

Chlorophyll Fluorescence Measurements and Analyses

A dual-wavelength pulse-amplitude-modulated (PAM) fluorescence monitoring system (Dual-PAM-100, Walz, Effeltrich, Germany) was employed to simultaneously measure the performance of PSII and PSI. To avoid the effect of phycobiliproteins on chlorophyll fluorescence, blue light (440 nm) was used as excitation light in the following measurements. Rapid fluorescence induction kinetics (Kautsky curves) showed a typical polyphasic rise pattern between O (the minimum fluorescence) and P (the maximum fluorescence) during the first second of illumination (Neubauer and Schreiber, 1987). The typical Kaustsky curve plotted against a logarithmic time scale represented different processes of photosynthetic electron transport (**Supplementary Figure S1**). According to Strasser and Strasser (1995) and Guisse et al. (1995), the fluorescence characterized of several different phases, where the time-specific steps were labeled as O, K (at ~300 μs), J (at ~2 ms), I (at ~30 ms) and P. Fluorescence intensities at different phases were noted as F_o, F_k, F_J, F_I and F_m. The standardized fluorescence intensity from the O- to P-phase was calculated as $V_t = (F_t - F_o)/(F_m - F_o)$. To assess the donor side activity of PSII, the normalized variable fluorescence at the K-step relative to the amplitude of $F_J - F_o$ (W_k) was calculated as $W_k = (F_k - F_o)/(F_J - F_o)$. To evaluate the activity of PSII, the maximum quantum yield of PSII (F_v/F_m) was calculated as $F_v/F_m = (F_m - F_o)/F_m$. The acceptor side activity of PSII, i.e., the probability that a trapped exciton moves an electron into the electron transport chain beyond Q_A^- (ψ_{ET2O}) and the quantum yield of electron transport (φ_{Eo}) was calculated as $\psi_{ET2O} = 1 - V_J$ and $\varphi_{Eo} = (1 - F_o/F_m) \times (1 - V_J)$, respectively. The redox state of inter-photosystem electron carriers and the acceptor side activity of PSI, i.e., the probability that an electron moves from reduced Q_A beyond PSI (ψ_{RE1O}), and the quantum yield for reduction of the end electron acceptors on the PSI acceptor side (φ_{Ro}), were calculated as $\psi_{RE1O} = 1 - V_I$ and $\varphi_{Ro} = (1\text{-}F_o/F_m) \times (1 - V_I)$, respectively. All these parameters were derived from JIP-tests (Strasser and Strasser, 1995; Strasser et al., 2004). According to the theory of energy fluxes in biomembranes (Strasser, 1981), the density of the PSII reaction

center per excited cross section (RC/CSo), the absorbed flux (ABS), the trapping flux (TRo), the electron transport flux (ETo), and the dissipated energy flux (DIo) by active reaction centers were calculated as.

$$RC/CSo = F_v/F_m \times V_J/V_K/4 \times F_O,$$
$$ABS/RC = 4 \times (F_K - F_O) \times F_m/(F_J - F_O) \times F_v,$$
$$TRo/RC = 4 \times (F_K - F_O)/(F_I - F_O),$$
$$ETo/RC = 4 \times (F_K - F_O) \times (F_m - F_J)/(F_J - F_O) \times F_v$$

and

$$DIo/RC = ABS/RC - TRo/RC.$$

P700 Measurements and Analyses

As suggested by Klughammer and Schreiber (1994), the $P700^+$ signal measured with the dual-wavelength (830/875 nm) unit of the instrument was taken as a measure of the redox state of P700. After 10 s exposure to far-red light, a saturation flash was applied to determine the maximum $P700^+$ signal (P_m). The steady-state $P700^+$ signal (P) was monitored under actinic light generated by the instrument at similar PAR levels as the natural sunlight (~800 μmol photons m^{-2} s^{-1}). The 0.8 s saturating flash of ~10, 000 μmol photons m^{-2} s^{-1} was applied to induce the maximum $P700^+$ value (P_m'). The effective quantum yield of PSI (YI) was calculated as $(P_m' - P)/P_m$.

In *Pyropia* spp., several published papers have demonstrated that the CET around PSI could account for up to 97.7% of total electron flow when algal blades suffered from severe desiccation (Gao and Wang, 2012). This was thus supposed to be one of the most important alternative electron transport pathway during exposure to stresses (Gao et al., 2013; Yu et al., 2018). Accordingly, our present study paid more attention on the physiological role of CET during the exposure to UVR and high-CO_2 induced OA. CET around PSI was evaluated by the measurement of the re-reduction kinetics of $P700^+$. After ~10 s exposure to far-red light, the applied saturation flash drives $P700^+$ to combine with electrons, and the initial linear slope of the re-reduction of $P700^+$ indicated the activity of CET.

All measured and calculated parameters are summarised in **Table 1**.

Statistical Analyses

In the present study, UVR-induced inhibition for a particular parameter was calculated as $(P_{PAR} - P_{PAR+UVR})/P_{PAR} \times 100\%$, where P_{PAR} and $P_{PAR+UVR}$ represent the values of the physiological parameter for the thalli grown under PAR alone or PAR + UVR, respectively. UVB-induced inhibition was derived from the difference in the values between the PAB (PAR + UVA + B) and PA (PAR + UVA) treatments.

Statistical analyses were performed using SPSS 19.0 (SPSS Inc., Chicago, IL, United States). The homogeneity of variance was examined using Levene's test before all statistical analyses. One-way ANOVA and *t*-test were used to establish differences among treatments. A two-way ANOVA was used to identify the effects of CO_2 concentration, light, UV, and their interactions. Differences were considered to be statistically significant at $p < 0.05$.

TABLE 1 | Measured and calculated parameters used in this paper.

Parameters	Physiological interpretation
Kautsky curves	
F_o, F_k, F_J, F_I, F_P	fluorescence intensity at O, K, J, I, P phases
V_t	relative variable fluorescence at time *t*
$W_k = (F_k - F_o)/(F_J - F_o)$	normalized variable fluorescence at the K-step relative to the amplitude of $F_J - F_o$
$F_v/F_m = (F_m - F_o)/F_m$	maximum photochemical efficiency of PSII
$RC/CS_o = F_v/F_m \times V_J/V_K/4 \times F_o$	density of PSII RC per excited cross sections
$\psi_{ET2O} = 1 - V_J$	probability that a trapped excition moves an electron into the electron transport chain beyond Q_A^-
$\varphi_{Eo} = (1 - F_o/F_m) \times (1 - V_J)$	quantum yield of electron transport
$\psi_{RE1O} = 1 - V_I$	probability that an electron moves from reduced Q_A beyond PSI
$\varphi_{Ro} = (1 - F_o/F_m) \times (1 - V_I)$	quantum yield for reduction of the end electron acceptors on the PSI acceptor side
$ABS/RC = 4 \times (F_k - F_o) \times F_m/(F_J - F_o) \times F_v$	absorbed flux by active RCs
$TR_o/RC = 4 \times (F_k - F_o)/(F_I - F_o)$	trapping flux by active RCs
$ET_o/RC = 4 \times (F_k - F_o) \times (F_m - F_J)/(F_J - F_o) \times F_v$	electron transport flux by active RCs
$DI_o/RC = ABS/RC - TR_o/RC$	dissipated energy flux by active RCs
P700 measurements	
P, P_m, P_m'	real-time, maximum, and maximum steady state, absorption signal of $P700^+$
$YI = (P_m' - P)/P_m$	effective photochemical quantum yield of PSI
$P700^+$ re-reduction	the activity of cyclic electron transport (CET) around PSI

PSII, photosystem II; PSI, photosystem I; RC, reaction center; CS, cross section.

RESULTS

Under the ambient CO_2 conditions (low-CO_2), the presence of UVR significantly inhibited the O_2-evolving complex (OEC) of PSII activities as evidenced by an increase of the variable fluorescence at the K-step of the Kautsky curve relative to the amplitude of $F_J - F_O$ (W_k; *t*-test, $p < 0.05$; **Figure 1**) and a decrease of the maximum quantum yield of PSII (F_v/F_m; *t*-test, $p < 0.05$; **Figure 2**). Furthermore, UVB-induced inhibition of the OEC, with an amplitude of up to ~24%, was significantly higher than that induced by UVA (~16%; *t*-test, $p < 0.05$). In contrast, the PSII acceptor side activity (ψ_{ET2O}; **Figure 3A**), quantum yield of electron transport (φ_{Eo}; **Figure 3B**), PSI donor side activity (ψ_{RE1O}; **Figure 3C**), and quantum yield for reduction of PSI acceptor side (φ_{Ro}; **Figure 3D**) were significantly increased by UVR, as shown here by the negative inhibition values (*t*-test, $p < 0.05$ for these four parameters). However, under the low-CO_2 conditions, the effective quantum yield of PSI showed no significant change (*t*-test, $p = 0.487$; **Figure 4**) between PAR and PAR + UVR treatments, indicating that PSI activity was less affected by UVR. However, an increase in the re-reduction rate of $P700^+$ showed that UVR significantly stimulated the activity of CET around PSI, especially in the presence of UVB,

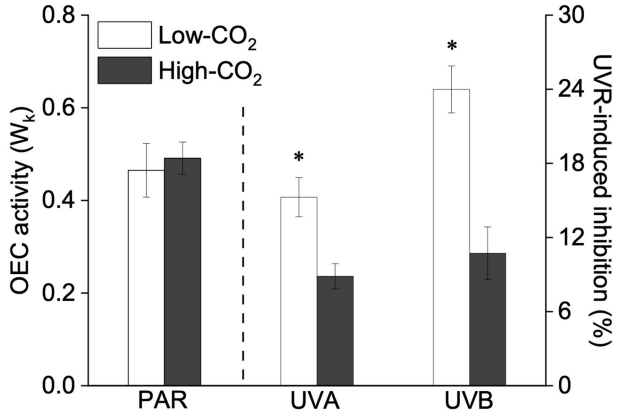

FIGURE 1 | Values (a.u., left pair of bars) and UVR-induced inhibition (%, right two pairs of bars) on the O_2-evolving complex (OEC) activity (the normalized variable fluorescence at the K-step relative to the amplitude of F_J–F_o, W_k) of *Pyropia yezoensis* growing for 9 days at low (~400 μatm, open bars) and high (~1000 μatm, closed bars) CO_2 conditions. Data are means ± *SD* ($n = 3$). The symbol "*" indicates a significant ($p < 0.05$, *t*-tests) difference between the treatments in each pair.

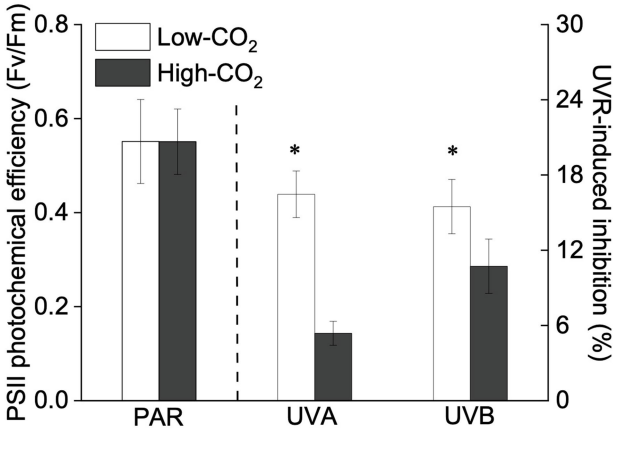

FIGURE 2 | Values (a.u., left pair of bars) and UVR-induced inhibition (%, right two pairs of bars) of PSII photochemical efficiency (F_v/F_m) of *P. yezoensis* growing for 9 days at low (~400 μatm, open bars) and high (~1000 μatm, closed bars) CO_2 conditions. Data are means ± *SD* ($n = 3$). The symbols "*" indicates a significant ($p < 0.05$, *t*-tests) difference between the treatments in each pair.

with increasing amplitude by up to ~17% (~7% for UVA and ~10% for UVB, respectively; *t*-test, $p < 0.05$ for both UVA and UVB treatments; **Figure 5**). Due to the fact that CET relates to electron transport rate in both PSII and PSI [as it could be calcultated by the difference between ETRI and ETRII (Yamori et al., 2011; Gao and Wang, 2012)], the asynchronous variation between PSI activity and CET was mainly attributed to the decrease of PSII photochemical efficiency. The active CET thus compensates for the loss of linear electron transport rate, maintaining a high efficiency of generating ATP. Analyses of the specific energy fluxes of PSII showed that UVR significantly inhibited the density of PSII reaction centers (RC/CSo), the absorbed photon flux (ABS), the trapping photon flux (TRo) and the electron transport flux (ETo; *t*-test, $p < 0.05$ for these four parameters), while there was an up-regulation of the dissipated energy flux (DIo; *t*-test, $p < 0.05$; **Figure 6**).

In the future-simulated high-CO_2 conditions, leading also to ocean acidification (OA), PAR alone did not induce any significant changes in W_k and F_v/F_m (*t*-test, $p = 0.378$ and 0.523, respectively; **Figures 1, 2**), indicating that both OEC and PSII were unaffected. The enhancements of ψ_{ET2O} (**Figure 3A**), φ_{Eo} (**Figure 3B**), ψ_{RE1O} (**Figure 3C**), and φ_{Ro} (**Figure 3D**) suggested that more electrons were transferred through the intersystem electron carriers under OA (*t*-test, $p < 0.05$ for these four parameters). Regarding the downstream electron transport chain, YI (**Figure 4**) and re-reduction rate of $P700^+$ (**Figure 5**) increased by up to ~11% and ~23%, respectively, implying an up-regulation in PSI and CET (*t*-test, $p < 0.05$ for these two parameters). Changes of the specific energy fluxes of PSII indicated the efficiency of active PSII reaction centers were enhanced by OA (*t*-test, $p < 0.05$; **Figure 6**).

A two-way ANOVA analysis showed that both CO_2 concentration, UVR, and their interaction, significantly affected OEC, PSII, the intersystem electron transport and CET activities, but not always PSI (**Table 2**). Under the high CO_2 condition, UVR-induced inhibition of both OEC and PSII photochemical efficiency significantly decreased, with UVA- and UVB-induced inhibition of OEC decreased from ~15% to ~9%, and from ~24% to ~11%, respectively (*t*-test, $p < 0.05$ for both UVA and UVB treatment); that of PSII by UVA and UVB ranged from ~16% to ~5%, and from ~15% to ~10%, respectively (*t*-test, $p < 0.05$ for both UVA and UVB treatment; **Figures 1, 2**). Although the extent of UVR-induced inhibition on ψ_{ET2O}, φ_{Eo}, ψ_{RE1O}, and φ_{Ro} exhibited significant differences between low- and high-CO_2 conditions (**Figure 3**), the absolute values of these parameters were less affected (*t*-test, $p = 0.647$, 0.548, 0.398 and 0.712 respectively). The significant difference in $P700^+$ re-reduction between low- and high-CO_2 indicated that there was a synergistic effect between increased CO_2/OA and UVR, the high-CO_2 further enhanced CET activity by up to ~4% and ~5% under the influences of UVA and UVB, respectively (*t*-test, $p < 0.05$ for both UVA and UVB treatment; **Table 2, Figure 5**). In PSII, UVR-induced inhibition on the density of PSII reaction centers (RC/CSo), the absorbed photon flux (ABS), the trapping photon flux (TRo), and the electron transport flux (ETo) was alleviated by the high-CO_2 treatment (*t*-test, $p < 0.05$ for both UVA and UVB treatment; **Figure 6**). Meanwhile, UVR-induced up-regulation of dissipated energy flux (DIo) was further enhanced under the high-CO_2/OA condition (*t*-test, $p < 0.05$ for both UVA and UVB treatment; **Figure 6**).

DISCUSSION

Our results suggest that in the red algae *P. yezoensis* (Ueda) M. S. Hwang and H. G. Choi, future elevated CO_2 and ocean acidification (OA) can alleviate both UVB- and UVA-induced inhibition on PSII by modulating the synergy between PSII

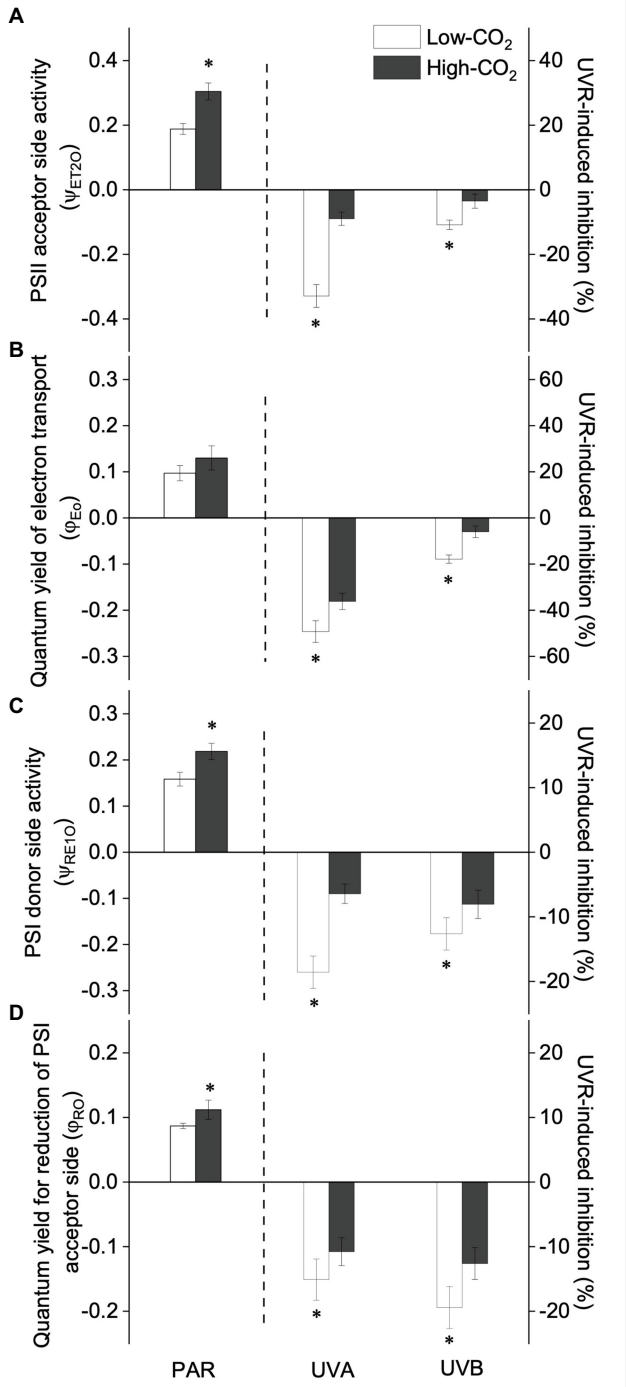

FIGURE 3 | Values (a.u., left pair of bars) and UVR-induced inhibition (%, right two pairs of bars) of PSII acceptor side activity [the probability that trapped excitons move electrons into the electron transport chain beyond Q_A^-, Ψ_{ET2O}, panel **(A)**], quantum yield of electron transport [φ_{Eo}, panel **(B)**], PSI donor side activity [the probability that an electron moves from reduced Q_A beyond PSI, Ψ_{RE1O}, panel **(C)**] and the quantum yield for reduction of PSI acceptor side [φ_{Ro}, panel **(D)**] of *P. yezoensis* growing for 9 days at low (~400 μatm, open bars) and high (~1000 μatm, closed bars) CO_2 conditions. Data are means ± *SD* ($n = 3$). The symbols "*" indicates a significant ($p < 0.05$, *t*-tests) difference between the treatments in each pair.

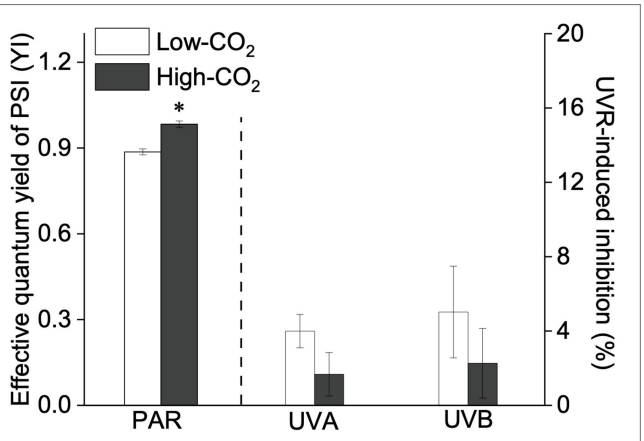

FIGURE 4 | Values (a.u., left pair of bars) and UVR-induced inhibition (%, right two pairs of bars) of the effective quantum yield of PSII (YI) of *P. yezoensis* growing for 9 days at low (~400 μatm, open bars) and high (~1000 μatm, closed bars) CO_2 conditions. Data are means ± *SD* ($n = 3$). The symbols "*" indicates a significant ($p < 0.05$, *t*-tests) difference between the treatments in each pair.

and PSI. Such synergy was found to relate mainly to the up-regulation of the intersystem electron transport efficiencies and CET around PSI (see **Figure 7**). In contrast with high-light-induced over-reduction of inter-photosystem electron transfer carriers (**Figure 7A**), UVR (especially UVB)-induced photoinhibition, characterized by the inhibition of OEC and PSII (**Figure 7B**), significantly decreased its quantum yield (**Figure 2**), which should be responsible for the reduced rates of carbon assimilation and growth (**Figure 7B**; Zhang et al., 2020). When grown and acclimated in the high-CO_2 condition (**Figure 7C**), the well- established coordination between PSII and PSI, as well as the enhanced CET around PSI sustain the efficient electron transport, consequently increasing the resilience of *P. yezoensis* to PAR and/or UVR.

Previous studies have shown that the presence of UVR would reduce primary productivity in cyanobacteria and of phytoplankton assemblages by about 20% due to the concomitant photoinhibition (Helbling et al., 2003; Neale and Thomas, 2017; Williamson et al., 2019). In our previous study (Zhang et al., 2020), UVR-induced growth inhibition of *P. yezoensis* was ~31%, with only about 5% being attributable to UVB, implying that UVR-induced loss of carbon fixation was mainly driven by the negative effects of UVA. However, here, we show that both UVA and UVB significantly inhibited the OEC and PSII, and the presence of UVB markedly exacerbated photoinhibition by 24% for OEC and 15% for PSII (**Figures 1, 2**). Macroalgae have evolved several adaptive mechanisms to cope with photoinhibition, by increasing NPQ and UVACs(Gao and Xu, 2008; Zheng and Gao, 2009; Zhang et al., 2020), enhancing the xanthophyll cycle (Häder et al., 2002; Aigner et al., 2017; Xie et al., 2020) as well as antioxidant systems (Sureda et al., 2008; Li et al., 2010). In the present work, the responses of photosynthetic electron transport to UVR (UVA and UVB) and the related modulations between the photosystems are

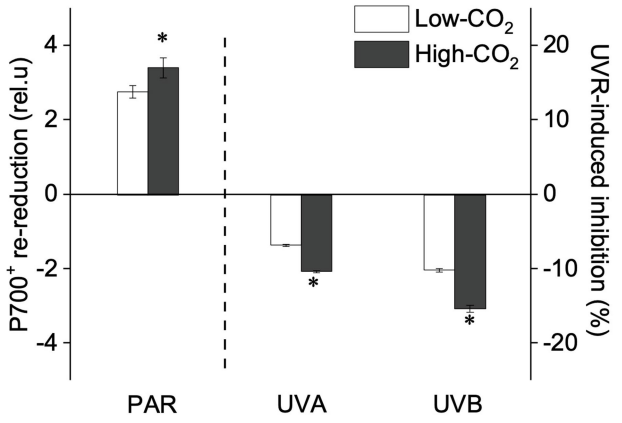

FIGURE 5 | Values (a.u., left pair of bars) and UVR-induced inhibition (%, right two pairs of bars) of CET activity (the $P700^+$ re-reduction rate) of *P. yezoensis* growing for 9 days at low (~400 μatm, open bars) and high (~1000 μatm, closed bars) CO_2 conditions. Data are means ± *SD* ($n = 3$). The symbols "*" indicates a significant ($p < 0.05$, *t*-tests) difference between the treatments in each pair.

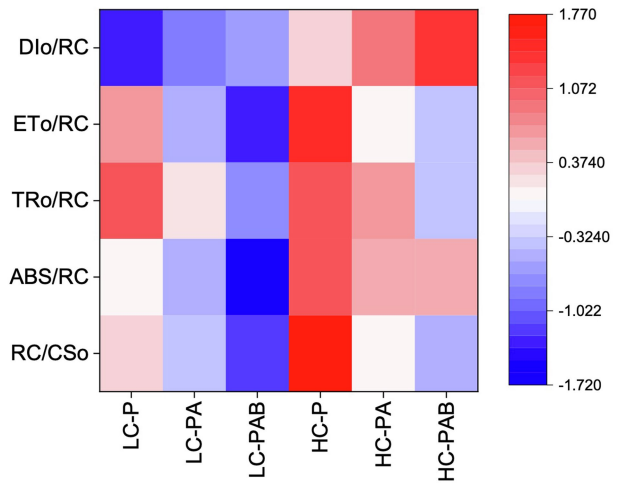

FIGURE 6 | Variations in the density of the PSII reaction centers per excited cross section (RC/CSo) and the specific energy fluxes [the absorbed flux (ABS/RC), the trapping flux (TRo/RC), the electron transport flux (ETo/RC), and the dissipated energy flux (DIo/RC)] of *P. yezoensis* growing for 9 days. LC and HC stand for low (~400 μatm) and high (~1000 μatm) CO_2 conditions, respectively. P, PA, and PAB stand for PAR only, PAR + UVA, and PAR + UVA + UVB, respectively.

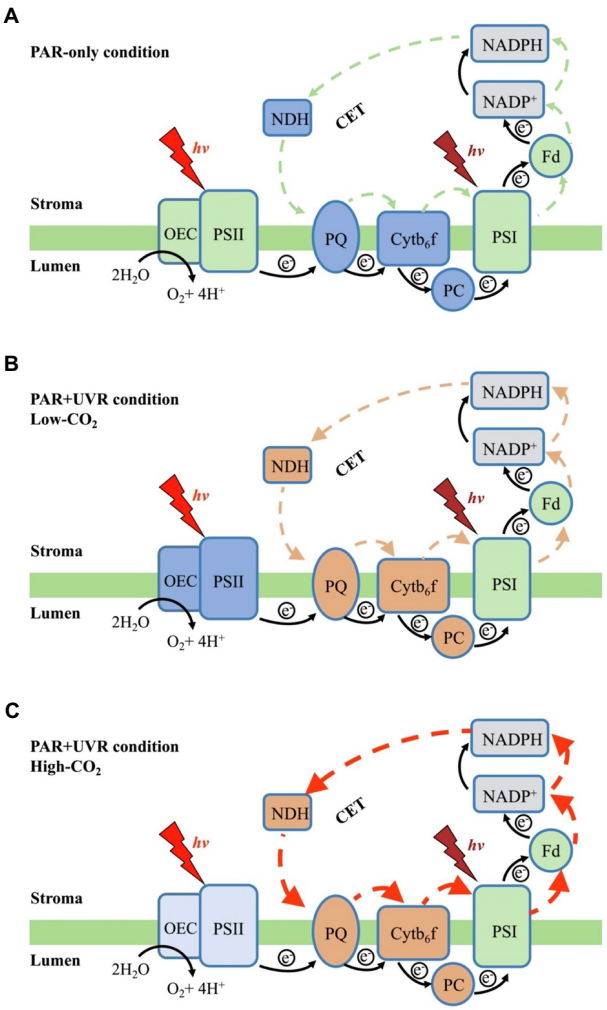

FIGURE 7 | Schematic representation of the coordination in *P. yezoensis* photosynthetic electron transport when exposed to PAR-only **(A)**, or to PAR + UVR under low-CO_2 **(B)** or high-CO_2 **(C)** concentrations. The green area indicates a normal state, the dark blue areas indicated a more severe inhibition, the light blue indicates a moderate inhibition, the orange area indicates an up-regulation, and the gray areas represent the unmeasured sites. Black arrows indicate linear electron transport flow, the colored arrows CET around PSI and the orange/red arrows indicate the up-regulation of CET.

speculated to be responsible for the observed asymmetric responses between photoinhibition and growth.

Under the influence of UVR, the deactivation of OEC would lower the efficiency of water splitting, and thus the excess excitation energy would also result in an accumulation of ROS, as well as $P680^+$ (Turcsányi and Vass, 2000; Tyystjärvi, 2008). These oxidized components can damage the D1 protein and lead to PSII photoinhibition (Zsiros et al., 2006). Our present study suggested that UVR inhibited the catalytic manganese cluster of the water-oxidizing complex, which has also been shown in other photosynthetic organisms (Vass et al., 1996; Turcsányi and Vass, 2000). Such damages are correlated with decreased O_2 evolution in the tested species of *Pyropia* (**Supplementary Table S1**, Figueroa et al., 1997; Aguilera et al., 1999, 2008). Nevertheless, such photoinhibition could lower electron transport from PSII to PSI and thus protect the intersystem electron carriers and PSI from over-reduction and alleviating PSI from photoinhibition (**Figures 4, 5, 7C**; as suggested also by Larosa et al., 2018).

In view of the impacts of increased CO_2 and OA, a number of previous studies have shown that high CO_2/OA treatments did benefit O_2 evolution and carbon assimilation in *Pyropia* spp. (**Supplementary Table S2**, Gao et al., 1991; Mercado et al.,

TABLE 2 | Two-way ANOVA for the effects of CO_2 (~400 and ~ 1,000 μatm) and irradiance quality photosynthetically active radiation (PAR, PAR + UVA and PAR + UVA + UVB) on the OEC activity (W_k), photosystem II (PSII) photochemical efficiency (F_v/F_m), intersystem electron transport efficiencies (ψ_{ET2O}, φ_{Eo}, ψ_{RE1O}, φ_{Ro}), photosystem I (PSI) activity (YI) and CET activity ($P700^+$ re-reduction).

	Irradiance quality		CO_2		Irradiance quality × CO_2	
	F	***p***	**F**	***p***	**F**	***p***
OEC activity (W_k)	45.06	<0.001	12.89	0.004	5.72	0.018
PSII photochemical efficiency (F_v/F_m)	354.51	<0.001	21.52	0.001	5.38	0.021
PSII acceptor side activity (ψ_{ET2O})	32.17	<0.001	34.66	<0.001	8.73	0.005
Quantum yield of electron transport (φ_{Eo})	7.33	0.008	49.49	<0.001	4.90	0.028
PSI donor side activity (ψ_{RE1O})	79.26	<0.001	13.24	0.003	5.28	0.023
Quantum yield for reduction of PSI acceptor side (φ_{Ro})	5.58	0.019	26.87	<0.001	4.39	0.037
Effective quantum yield of PSI (YI)	1.94	0.186	22.12	0.001	0.70	0.515
CET activity ($P700^+$ re-reduction)	23.46	<0.001	146.14	<0.001	4.63	0.032

1999; Chen et al., 2016, 2017; Zhang et al., 2020). Our results showed here that both OEC and PSII of *P. yezoensis* were less affected under PAR-only conditions, with PSI and CET being significantly up-regulated (**Figures 4, 5**). In contrast to the donor side photoinhibition induced by UVR, high-light induced photoinhibition is usually related to the over-reduction of intersystem electron carriers (Vass et al., 2005; Tyystjärvi, 2008). In the present work, the enhancement of CET would work as an alternative electron flow sink, together with the oxidized PSI, promoting the intersystem electron carriers to become oxidized, as reflected in negative inhibition (i.e., enhancement; **Figure 3**). Moreover, the up-regulated CET could also regulate the energy balance by consuming NADPH and generating ATP; $NADP^+$ can also accept more electrons transferred from PSII and then oxidize the intersystem electron carriers (as suggested by Bukhov and Carpentier, 2004; Rumeau et al., 2007; Gao and Wang, 2012; Yu et al., 2018), thus contributing to the supply of energy for carboxylation.

The interactive effects of UVR and CO_2 enrichment have been previously reported to be species-specific and UV-intensity-dependent (Gordillo et al., 2015; Ji and Gao, 2020 and references therein). A moderate UVR exposure amplified the positive effects of CO_2 and OA on the red coralline algae *Corallina officinalis* under low PAR (Yildiz et al., 2013), while the synergistic effect of incident solar UVR and OA resulted in a decrease in both photosynthesis and calcification of the coralline algae *Corallina sessilis* (Gao and Zheng, 2010). In *P. yezoensis*, our results suggested that the increased CO_2 and associated OA alleviated UVR-induced inhibition of the photosynthetic processes. Under the high-CO_2 conditions, the up-regulation of CET would generate a higher trans-thylakoid proton gradient (ΔpH), which increase NPQ and could produce ATP for carbon assimilation. Moreover, the higher ΔpH-induced acidification of the lumen could also drive a Ca^{2+}/H^+ antiport to sequester Ca^{2+} into the lumen (Krieger and Weis, 1993; Ettinger et al., 1999), and thus aid in maintaining OEC stability, as reflected by our data showing alleviation of UVR-induced OEC inhibition by high CO_2 treatments (**Figure 1**). Accordingly, OEC inhibition-induced photo-oxidative damage was significantly decreased, as evidenced by the increase of PSII photochemical efficiency (**Figure 2**), as well as the enhancement of the efficiency of the active PSII reaction center (**Figure 6**). Similar response was also observed in a tropical tree species (Huang et al., 2016) and marine angiosperm (Tan et al., 2020).

As mentioned above, the elevated DIC/CO_2 in seawater can down-regulate the CCMs, which is also true for *P. yezoensis* (Li et al., 2016). However, little attention has been paid to the effects of high PAR/UVR as well as its combined effects with high CO_2-induced OA. According to several published papers, high PAR/UVR affects the CCMs in different ways, and the effect is species-specific and light intensity dependent. For example, UVR enhanced the activity of extracellular carbonic anhydrase in *Skeletonema costatum* and thus enhanced its CCM (Wu and Gao, 2009), while a short-term exposure to UVR did not affect the inorganic carbon acquisition in *Dunaliella tertiolecta* (Beardall et al., 2002). Considering the fact that inorganic carbon acquisition is the prerequisite for carbon assimilation, which is the main photosynthetic electron sink, investigations of CCMs under high PAR/UVR and high CO_2 are expected in future studies.

Under natural conditions in sea-farming areas, macroalgae experience low pH and high CO_2 during the early morning period due to respiratory CO_2 release at night. Our results imply that the red algae *P. yezoensis* can take advantage of the concomitant changes in the pCO_2 and pH to cope with increasing UV exposure following sunrise. In addition, progressive OA associated with CO_2 rise could positively enhance the alga's photosynthesis and growth even under the influences of UVR, owing to the modulated synergy between PSII and PSI.

DATA AVAILABILITY STATEMENT

The raw data supporting the conclusions of this article will be made available by the authors, without undue reservation.

AUTHOR CONTRIBUTIONS

DZ: conceptualization, data collection and curation, data analysis, visualization, writing – original draft, and review and editing. JX: data collection and curation and review and editing. SB and JB: data analysis, formal analysis, and writing – review and editing. CZ: formal analysis and writing – review and editing. KG: conceptualization, funding acquisition, project administration, writing – original draft, and review and editing. All authors contributed to the article and approved the submitted version.

FUNDING

This study was supported by the National Natural Science Foundation (41720104005, 41721005, and 41890803).

ACKNOWLEDGMENTS

We are grateful to Xianglan Zeng and Wenyan Zhao for their technical assistance.

SUPPLEMENTARY MATERIAL

The Supplementary Material for this article can be found online at: https://www.frontiersin.org/articles/10.3389/fpls.2021.726538/full#supplementary-material

REFERENCES

Aguilera, J., Figueroa, F. L., Häder, D. P., and Jiménez, C. (2008). Photoinhibition and photosynthetic pigment reorganisation dynamics in light/darkness cycles as photoprotective mechanisms of *Porphyra umbilicalis* against damaging effects of UV radiation. *Sci. Mar.* 72, 87–97. doi: 10.3989/scimar.2008.72n187

Aguilera, J., Jiménez, C., Figueroa, F. L., Lebert, M., and Häder, D. P. (1999). Effect of ultraviolet radiation on thallus absorption and photosynthetic pigments in the red alga *Porphyra umbilicalis*. *J. Photochem. Photobiol. B* 48, 75–82. doi: 10.1016/S1011-1344(99)00015-9

Aigner, S., Holzinger, A., Karsten, U., and Kranner, I. (2017). The freshwater red alga *Batrachospermum turfosum* (Florideophyceae) can acclimate to a wide range of light and temperature conditions. *Eur. J. Phycol.* 52, 238–249. doi: 10.1080/09670262.2016.1274430

Aline, T., Atkinson, M. J., and Christopher, L. (2006). Effects of elevated pCO_2 on epilithic and endolithic metabolism of reef carbonates. *Glob. Chang. Biol.* 12, 2200–2208. doi: 10.1111/j.1365-2486.2006.01249.x

Andría, J. R., Brun, F. G., Pérez-Lloréns, J. L., and Vergara, J. J. (2001). Acclimation responses of *Gracilaria* sp. (Rhodophyta) and *Enteromorpha intestinalis* (Chlorophyta) to changes in the external inorganic carbon concentration. *Bot. Mar.* 44, 361–370. doi: 10.1515/BOT.2001.046

Andría, J., Vergara, J., and Pérez-Lloréns, J. L. (1999). Biochemical responses and photosynthetic performance of *Gracilaria* sp. (Rhodophyta) from Cádiz, Spain, cultured under different inorganic carbon and nitrogen levels. *Eur. J. Phycol.* 34, 497–504.

Beardall, J., Heraud, P., Roberts, S., Shelly, K., and Stojkovic, S. (2002). Effects of UV-B radiation on inorganic carbon acquisition by the marine microalga *Dunaliella tertiolecta* (Chlorophyceae). *Phycologia* 41, 268–272. doi: 10.2216/i0031-8884-41-3-268.1

Beer, S., and Koch, E. (1996). Photosynthesis of marine macroalgae and seagrasses in globally changing CO_2 environments. *Mar. Ecol. Prog. Ser.* 141, 199–204. doi: 10.3354/meps141199

Blouin, N. A., Brodie, J. A., Grossman, A. C., Xu, P., and Brawley, S. H. (2011). *Porphyra*: a marine crop shaped by stress. *Trends Plant Sci.* 16, 29–37. doi: 10.1016/j.tplants.2010.10.004

Büdenbender, J., Riebesell, U., and Form, A. (2011). Calcification of the Arctic coralline red algae *Lithothamnion glaciale* in response to elevated CO_2. *Mar. Ecol. Prog. Ser.* 441, 79–87. doi: 10.3354/meps09405

Bukhov, N., and Carpentier, R. (2004). Alternative photosystem I-driven electron transport routes: mechanisms and functions. *Photosynth. Res.* 82, 17–33. doi: 10.1023/B:PRES.0000040442.59311.72

Chen, B., Zou, D., and Ma, J. (2016). Interactive effects of elevated CO_2 and nitrogen–phosphorus supply on the physiological properties of *Pyropia haitanensis* (Bangiales, Rhodophyta). *J. Appl. Phycol.* 28, 1235–1243. doi: 10.1007/s10811-015-0628-z

Chen, B., Zou, D., and Yang, Y. (2017). Increased iron availability resulting from increased CO_2 enhances carbon and nitrogen metabolism in the economical marine red macroalga *Pyropia haitanensis* (Rhodophyta). *Chemosphere* 173, 444–451. doi: 10.1016/j.chemosphere.2017.01.073

Eberhard, S., Finazzi, G., and Wollman, F. A. (2008). The dynamics of photosynthesis. *Annu. Rev. Genet.* 42, 463–515. doi: 10.1146/annurev.genet.42.110807.091452

Ettinger, W. F., Clear, A. M., Fanning, K. J., and Peck, M. L. (1999). Identification of a Ca^{2+}/H^+ antiport in the plant chloroplast thylakoid membrane. *Plant Physiol.* 119, 1379–1386. doi: 10.1104/pp.119.4.1379

Figueroa, F. L., Salles, S., Aguilera, J., Jiménez, C., Mercado, J., Viñegla, B., et al. (1997). Effects of solar radiation on photoinhibition and pigmentation in the red alga *Porphyra leucosticta*. *Mar. Ecol. Prog. Ser.* 151, 81–90. doi: 10.3354/meps151081

Gao, K., Aruga, Y., Asada, K., Ishihara, T., Akano, T., and Kiyohara, M. (1991). Enhanced growth of the red alga *Porphyra yezoensis* Ueda in high CO_2 concentrations. *J. Appl. Phycol.* 3, 355–362. doi: 10.1007/BF02392889

Gao, K., Aruga, Y., Asada, K., Ishihara, T., Akano, T., and Kiyohara, M. (1993). Calcification in the articulated coralline alga *Corallina pilulifera*, with special reference to the effect of elevated CO_2 concentration. *Mar. Biol.* 117, 129–132. doi: 10.1007/BF00346434

Gao, K., Beardall, J., Häder, D. P., Hall-Spencer, J. M., Gao, G., and Hutchins, D. A. (2019). Effects of ocean acidification on marine photosynthetic organisms under the concurrent influences of warming, UV radiation, and deoxygenation. *Front. Mar. Sci.* 6:322. doi: 10.3389/fmars.2019.00322

Gao, K., Guan, W., and Helbling, E. W. (2007). Effects of solar ultraviolet radiation on photosynthesis of the marine red tide alga *Heterosigma akashiwo* (Raphidophyceae). *J. Photochem. Photobiol. B* 86, 140–148. doi: 10.1016/j.jphotobiol.2006.05.007

Gao, S., Niu, J., Chen, W., Wang, G., Xie, X., Pan, G., et al. (2013). The physiological links of the increased photosystem II activity in moderately desiccated *Porphyra haitanensis* (Bangiales, Rhodophyta) to the cyclic electron flow during desiccation and re-hydration. *Photosynth. Res.* 116, 45–54. doi: 10.1007/s11120-013-9892-4

Gao, S., and Wang, G. (2012). The enhancement of cyclic electron flow around photosystem I improves the recovery of severely desiccated *Porphyra yezoensis* (Bangiales, Rhodophyta). *J. Exp. Bot.* 63, 4349–4358. doi: 10.1093/jxb/ers082

Gao, K., and Xu, J. (2008). Effects of solar UV radiation on diurnal photosynthetic performance and growth of *Gracilaria lemaneiformis* (Rhodophyta). *Eur. J. Phycol.* 43, 297–307. doi: 10.1080/09670260801986837

Gao, K., and Zheng, Y. (2010). Combined effects of ocean acidification and solar UV radiation on photosynthesis, growth, pigmentation and calcification of the coralline alga *Corallina sessilis* (Rhodophyta). *Glob. Chang. Biol.* 16, 2388–2398. doi: 10.1111/j.1365-2486.2009.02113.x

Gordillo, F. J., Aguilera, J., Wiencke, C., and Jiménez, C. (2015). Ocean acidification modulates the response of two Arctic kelps to ultraviolet radiation. *J. Plant Physiol.* 173, 41–50. doi: 10.1016/j.jplph.2014.09.008

Guisse, B., Srivastava, A., and Strasser, R. (1995). The polyphasic rise of the chlorophyll *a* fluorescence (OKJIP) in heat-stressed leaves. *Arch. Sci.* 48, 147–160. doi: 10.5169/SEALS-740252

Häder, D. P., and Barnes, P. W. (2019). Comparing the impacts of climate change on the responses and linkages between terrestrial and aquatic ecosystems. *Sci. Total Environ.* 682, 239–246. doi: 10.1016/j.scitotenv.2019.05.024

Häder, D. P., Lebert, M., Sinha, R. P., Barbieri, E. S., and Helbling, E. W. (2002). Role of protective and repair mechanisms in the inhibition of photosynthesis in marine macroalgae. *Photochem. Photobiol. Sci.* 1, 809–814. doi: 10.1039/B206152J

Helbling, E. W., Gao, K., Gonçalves, R. J., Wu, H., and Villafañe, V. E. (2003). Utilization of solar UV radiation by coastal phytoplankton assemblages off SE China when exposed to fast mixing. *Mar. Ecol. Prog. Ser.* 259, 59–66. doi: 10.3354/meps259059

Huang, W., Yang, Y. J., Hu, H., Zhang, S. B., and Cao, K. F. (2016). Evidence for the role of cyclic electron flow in photoprotection for oxygen-evolving complex. *J. Plant Physiol.* 194, 54–60. doi: 10.1016/j.jplph.2016.02.016

Hurd, C. L., Beardall, J., Comeau, S., Cornwall, C. E., Havenhand, J. N., Munday, P. L., et al. (2020). Ocean acidification as a multiple driver: how interactions between changing seawater carbonate parameters affect marine life. *Mar. Freshw. Res.* 71, 263–274. doi: 10.1071/MF19267

IPCC (2014) in *Climate Change 2014: Synthesis Report. Contribution of Working Groups I, II and III to the Fifth Assessment Report of the Intergovernmental Panel on Climate Change*. eds. Core Writing Team, R. K. Pachauri and L. A. Meyer (Geneva, Switzerland: IPCC), 151.

Ji, Y., and Gao, K. (2020). Effects of climate change factors on marine macroalgae: a review. *Adv. Mar. Biol.* 88, 91–136. doi: 10.1016/bs.amb.2020.11.001

Jiang, H., Gao, K., and Helbling, E. W. (2007). Effects of solar UV radiation on germination of conchospores and morphogenesis of sporelings in *Porphyra haitanensis* (Rhodophyta). *Mar. Biol.* 151, 1751–1759. doi: 10.1007/s00227-007-0632-1

Klughammer, C., and Schreiber, U. (1994). An improved method, using saturating light pulses, for the determination of photosystem I quantum yield via $P700^+$-absorbance changes at 830 nm. *Planta* 192, 261–268. doi: 10.1007/BF01089043

Korbee, N., Navarro, N. P., García-Sánchez, M., Celis-Plá, P. S. M., Quintano, E., Copertino, M. D. S., et al. (2014). A novel in situ system to evaluate the effect of high CO_2 on photosynthesis and biochemistry of seaweeds. *Aquat. Biol.* 22, 245–259. doi: 10.3354/ab00594

Krieger, A., and Weis, E. (1993). The role of calcium in the pH-dependent control of photosystem II. *Photosynth. Res.* 37, 117–130. doi: 10.1007/BF02187470

Larosa, V., Meneghesso, A., La Rocca, N., Steinbeck, J., Hippler, M., Szabò, I., et al. (2018). Mitochondria affect photosynthetic electron transport and photosensitivity in a green alga. *Plant Physiol.* 176, 2305–2314. doi: 10.1104/pp.17.01249

Li, X., Xu, J., and He, P. (2016). Comparative research on inorganic carbon acquisition by the macroalgae *Ulva prolifera* (Chlorophyta) and *Pyropia yezoensis* (Rhodophyta). *J. Appl. Phycol.* 28, 491–497. doi: 10.1007/s10811-015-0603-8

Li, L., Zhao, J., and Tang, X. (2010). Ultraviolet irradiation induced oxidative stress and response of antioxidant system in an intertidal macroalgae *Corallina officinalis* L. *J. Environ. Sci.* 22, 716–722. doi: 10.1016/S1001-0742(09)60168-6

Lu, X., Huan, L., Gao, S., Gao, S. (2016). NADPH from the oxidative pentose phosphate pathway drives the operation of cyclic electron flow around photosystem I in high-intertidal macroalgae under severe salt stress *Physiol. Plantarum.* 156, 397–406. doi: 10.1111/ppl.12383

Martin, S., and Gattuso, J. P. (2009). Response of Mediterranean coralline algae to ocean acidification and elevated temperature. *Glob. Chang. Biol.* 15, 2089–2100. doi: 10.1111/j.1365-2486.2009.01874.x

Mercado, J. M., Javier, F., Gordillo, L., Niell, F. X., and Figueroa, F. L. (1999). Effects of different levels of CO_2 on photosynthesis and cell components of the red alga *Porphyra leucosticta*. *J. Appl. Phycol.* 11, 455–461. doi: 10.1023/A:1008194223558

Miyake, C. (2010). Alternative electron flows (water–water cycle and cyclic electron flow around PSI) in photosynthesis: molecular mechanisms and physiological functions. *Plant Cell Physiol.* 51, 1951–1963. doi: 10.1093/pcp/pcq173

Neale, R. E., Barnes, P. W., Robson, T. M., Neale, P. J., Williamson, C. E., Zepp, R. G., et al. (2021). Environmental effects of stratospheric ozone depletion, UV radiation, and interactions with climate change: UNEP environmental effects assessment panel, update 2020. *Photochem. Photobiol. Sci.* 20, 1–67. doi: 10.1007/s43630-020-00001-x

Neale, P. J., and Thomas, B. C. (2017). Inhibition by ultraviolet and photosynthetically available radiation lowers model estimates of depth-integrated picophytoplankton photosynthesis: global predictions for *Prochlorococcus* and *Synechococcus*. *Glob. Chang. Biol.* 23, 293–306. doi: 10.1111/gcb.13356

Neubauer, C., and Schreiber, U. (1987). The polyphasic rise of chlorophyll fluorescence upon onset of strong continuous illumination: I. saturation characteristics and partial control by the photosystem II acceptor side. *Zeitschrift für Naturforschung C* 42, 1246–1254. doi: 10.1515/znc-1987-11-1217

Niu, J., Feng, J., Xie, X., Gao, S., and Wang, G. (2016). Involvement of cyclic electron flow in irradiance stress responding and its potential regulation of the mechanisms in *Pyropia yezoensis*. *Chin. J. Oceanol. Limnol.* 34, 730–739. doi: 10.1007/s00343-016-4236-9

Pierrot, D., Lewis, E., and Wallace, D. W. R. (2006). MS Excel program developed for CO_2 system calculations. ORNL/CDIAC-105a. *Environ. Sci.* doi: 10.3334/CDIAC/otg.CO2SYS_XLS_CDIAC105a

Raven, J. A., Beardall, J., and Giordano, M. (2014). Energy costs of carbon dioxide concentrating mechanisms in aquatic organisms. *Photosynth. Res.* 121, 111–124. doi: 10.1007/s11120-013-9962-7

Rumeau, D., Peltier, G., and Cournac, L. (2007). Chlororespiration and cyclic electron flow around PSI during photosynthesis and plant stress response. *Plant Cell Environ.* 30, 1041–1051. doi: 10.1111/j.1365-3040.2007.01675.x

Semesi, I. S., Kangwe, J., and Björk, M. (2009). Alterations in seawater pH and CO_2 affect calcification and photosynthesis in the tropical coralline alga, *Hydrolithon* sp. (Rhodophyta). *Estuar. Coast. Shelf Sci.* 84, 337–341. doi: 10.1016/j.ecss.2009.03.038

Strasser, R. J. (1981). "The grouping model of plant photosynthesis: heterogeneity of photosynthetic units in thylakoids," in *Photosynthesis III. Structure and Molecular Organisation of the Photosynthetic Apparatus*. ed. G. Akoyonoglou (Philadelphia: Balaban International Science Services), 727–737.

Strasser, B. J., and Strasser, R. J. (1995). "Measuring fast fluorescence transients to address environmental questions: The JIP-test," in *Photosynthesis: From Light to Biosphere*. ed. Mathis. Vol. 5 ed (Netherlands: Kluwer Academic Publishers), 977–980.

Strasser, R. J., Tsimilli-Michael, M., and Srivastava, A. (2004). "Analysis of the chlorophyll *a* fluorescence transient," in *Chlorophyll a Fluorescence*. eds. G. C. Papageorgiou and Govindjee (Dordrecht: Springer), 321–362.

Su, H. N., Xie, B. B., Zhang, X. Y., Zhou, B. C., and Zhang, Y. Z. (2010). The supramolecular architecture, function, and regulation of thylakoid membranes in red algae: an overview. *Photosynth. Res.* 106, 73–87. doi: 10.1007/s11120-010-9560-x

Suárez-Álvarez, S., Gómez-Pinchetti, J. L., and García-Reina, G. (2012). Effects of increased CO_2 levels on growth, photosynthesis, ammonium uptake and cell composition in the macroalga *Hypnea spinella* (Gigartinales, Rhodophyta). *J. Appl. Phycol.* 24, 815–823. doi: 10.1007/s10811-011-9700-5

Sureda, A., Box, A., Terrados, J., Deudero, S., and Pons, A. (2008). Antioxidant response of the seagrass Posidonia oceanica when epiphytized by the invasive macroalgae *Lophocladia lallemandii*. *Mar. Environ. Res.* 66, 359–363. doi: 10.1016/j.marenvres.2008.05.009

Tan, Y., Zhang, Q. S., Zhao, W., Liu, Z., Ma, M. Y., Zhong, M. Y., et al. (2020). The highly efficient NDH-dependent photosystem I cyclic electron flow pathway in the marine angiosperm *Zostera marina*. *Photosynth. Res.* 144, 49–62. doi: 10.1007/s11120-020-00732-z

Turcsányi, E., and Vass, I. (2000). Inhibition of photosynthetic electron transport by UV-A radiation targets the photosystem II complex. *Photochem. Photobiol.* 72, 513–520. doi: 10.1562/0031-8655(2000)072<0513:IOPETB>2.0.CO;2

Tyystjärvi, E. (2008). Photoinhibition of photosystem II and photodamage of the oxygen evolving manganese cluster. *Coord. Chem. Rev.* 252, 361–376. doi: 10.1016/j.ccr.2007.08.021

Vass, I., Sass, L., Spetea, C., Bakou, A., Ghanotakis, D. F., and Petrouleas, V. (1996). UV-B-induced inhibition of photosystem II electron transport studied by EPR and chlorophyll fluorescence. Impairment of donor and acceptor side components. *Biochemistry* 35, 8964–8973. doi: 10.1021/bi9530595

Vass, I., Szilárd, A., and Sicora, C. (2005). "Adverse effects of UV-B light on the structure and function of the photosynthetic apparatus," in *Handbook of Photosynthesis*. ed. Mohammad Pessarakli (Boca Raton, FL, USA: Francis and Taylor publisher), 43–63.

Viñegla, B., Segovia, M., and Figueroa, F. L. (2006). Effect of artificial UV radiation on carbon and nitrogen metabolism in the macroalgae *Fucus spiralis* L. and *Ulva olivascens* Dangeard. *Hydrobiologia* 560, 31–42. doi: 10.1007/s10750-005-1097-1

Williamson, C. E., Neale, P. J., Hylander, S., Rose, K. C., Figueroa, F. L., Robinson, S. A., et al. (2019). The interactive effects of stratospheric ozone depletion, UV radiation, and climate change on aquatic ecosystems. *Photochem. Photobiol. Sci.* 18, 717–746. doi: 10.1039/c8pp90062k

Wu, H., and Gao, K. (2009). Ultraviolet radiation stimulated activity of extracellular carbonic anhydrase in the marine diatom *Skeletonema costatum*. *Funct. Plant Biol.* 36, 137–143. doi: 10.1071/FP08172

Xie, X., Lu, X., Wang, L., He, L., and Wang, G. (2020). High light intensity increases the concentrations of β-carotene and zeaxanthin in marine red macroalgae. *Algal Res.* 47:101852. doi: 10.1016/j.algal.2020.101852

Xu, J., and Gao, K. (2008). Growth, pigments, UV-absorbing compounds and agar yield of the economic red seaweed *Gracilaria lemaneiformis* (Rhodophyta) grown at different depths in the coastal waters of the South China Sea. *J. Appl. Phycol.* 20, 681–686. doi: 10.1007/s10811-007-9247-7

Xu, J., and Gao, K. (2010). UV-A enhanced growth and UV-B induced positive effects in the recovery of photochemical yield in *Gracilaria lemaneiformis* (Rhodophyta). *J. Photochem. Photobiol. B* 100, 117–122. doi: 10.1016/j.jphotobiol.2010.05.010

Xu, J., and Gao, K. (2012). Future CO_2-induced ocean acidification mediates the physiological performance of a green tide alga. *Plant Physiol.* 160, 1762–1769. doi: 10.1104/pp.112.206961

Yamori, W., Sakata, N., Suzuki, Y., Shikanai, T., and Makino, A. (2011). Cyclic electron flow around photosystem I via chloroplast NAD (P) H dehydrogenase (NDH) complex performs a significant physiological role during photosynthesis and plant growth at low temperature in rice. *Plant J.* 68, 966–976. doi: 10.1111/j.1365-313X.2011.04747.x

Yildiz, G., Hofmann, L. C., Bischof, K., and Dere, Ş. (2013). Ultraviolet radiation modulates the physiological responses of the calcified rhodophyte *Corallina officinalis* to elevated CO_2. *Bot. Mar.* 56, 161–168. doi: 10.1515/bot-2012-0216

Yu, B., Niu, J., Feng, J., Xu, M., Xie, X., Gu, W., et al. (2018). Regulation of ferredoxin-$NADP^+$ oxidoreductase to cyclic electron transport in high salinity stressed *Pyropia yezoensis*. *Front. Plant Sci.* 9:1092. doi: 10.3389/fpls.2018.01092

Zhang, D., Xu, J., Bao, M., Yan, D., Beer, S., Beardall, J., et al. (2020). Elevated CO_2 concentration alleviates UVR-induced inhibition of photosynthetic light reactions and growth in an intertidal red macroalga. *J. Photochem. Photobiol. B* 213:112074. doi: 10.1016/j.jphotobiol.2020.112074

Zheng, Y., and Gao, K. (2009). Impacts of solar UV radiation on the photosynthesis, growth, and UV-absorbing compounds in *Gracilaria lemaneiformis* (Rhodophyta) grown at different nitrate concentrations. *J. Phycol.* 45, 314–323. doi: 10.1111/j.1529-8817.2009.00654.x

Zou, D. (2005). Effects of elevated atmospheric CO_2 on growth, photosynthesis and nitrogen metabolism in the economic brown seaweed, *Hizikia fusiforme* (Sargassaceae, Phaeophyta). *Aquaculture* 250, 726–735. doi: 10.1016/j.aquaculture.2005.05.014

Zou, D., and Gao, K. (2005). Ecophysiological characteristics of four intertidal marine macroalgae during emersion along Shantou coast of China, with a special reference to the relationship of photosynthesis and CO_2. *Acta Oceanol. Sin.* 24, 105–113.

Zou, D., Gao, K., and Xia, J. (2003). Photosynthetic utilization of inorganic carbon in the economic brown alga, *Hizikia Fusiforme* (Sargassaceae) from the South China Sea. *J. Phycol.* 39, 1095–1100. doi: 10.1111/j.0022-3646.2003.03-038.x

Zsiros, O., Allakhverdiev, S. I., Higashi, S., Watanabe, M., Nishiyama, Y., and Murata, N. (2006). Very strong UV-A light temporally separates the photoinhibition of photosystem II into light-induced inactivation and repair. *Biochim. Biophys. Acta* 1757, 123–129. doi: 10.1016/j.bbabio.2006.01.004

Conflict of Interest: The authors declare that the research was conducted in the absence of any commercial or financial relationships that could be construed as a potential conflict of interest.

Publisher's Note: All claims expressed in this article are solely those of the authors and do not necessarily represent those of their affiliated organizations, or those of the publisher, the editors and the reviewers. Any product that may be evaluated in this article, or claim that may be made by its manufacturer, is not guaranteed or endorsed by the publisher.